The L1457 Molecular/Atomic Cloud Complex: HI and CO Maps

G. H. Moriarty-Schieven
Dominion Radio Astrophysical Observatory, National Research Council, Box 248, Penticton, British Columbia, V2A 6K3, Canada & Joint Astronomy Centre, 660 N. A'ohoku Pl., Hilo, HI 96720 (gms@jach.hawaii.edu)

B-G Andersson and P. G. Wannier
Jet Propulsion Laboratory, MS 169-506, 4800 Oak Grove Dr., Pasadena, CA 91109 (bg@jplsp.jpl.nasa.gov, wannier@jplsp.jpl.nasa.gov)

ABSTRACT

L1457 is the closest known molecular cloud (65pc), and lies near the edge of the local hot bubble, and well out of the galactic plane ($b \sim -34°$). We have mapped an $8° \times 8°$region at 35' resolution, and a $3° \times 5°$region at ~2' resolution, in HI 21cm emission. We have also mapped a $2° \times 4°$region at 2' resolution in ^{12}CO J=1-0. We find that there is an extended component of atomic gas, clearly associated with the molecular complex, and comparable to it in total mass. The HI structure at small scales in the vicinity of the molecular clouds is remarkable, consisting largely of long, narrow filaments <20' (0.2pc) in width and 1°- 4°in length. A thin (<10') limb-brightened atomic halo is seen to surround the CO at some velocities, but is ill-defined at other velocities. The halo may be disturbed by external pressure, perhaps from the hot gas in the local bubble.

The molecular clouds are part of a large structure $\sim 5° \times 3°$in extent with a small "funnel-shaped" extension to the south. The structure, which we call the L1457 atomic/molecular complex, is dominated by HI in the north and H_2 in the south extension. Roughly half the mass of the complex is molecular. The structure of this complex at both large- and small-scale suggests that the south end has been recently compressed.

Subject headings: atomic data — ism: clouds — ism: individual (L1457) — ism: general — molecular data

1. Introduction

The interstellar medium (ISM) consists of several different components or "phases", including dust, molecular gas, neutral atomic gas, and ionized plasma, all of which coexist, interact, and change from one form to another. The local ISM ($\lesssim$ 100pc) has been characterized as a "bubble" of hot ionized gas giving rise to a soft X-ray background (McCammon et al., 1983; Cox & Reynolds, 1987; Welch et al. 1994). Near the edge of and possibly within this bubble are several high-latitude molecular clouds, among them the dark clouds L1453, L1454, L1457 and L1458 (Lynds 1963), which we will collectively call the L1457 molecular complex (see Figure 1). Located well out of the galactic plane ($b \sim -34°$), this complex is relatively uncontaminated by background HI or CO emission.

Hobbs et al. (1986, 1988) have been able to put strong constraints on the distance to the north part of the molecular complex of between 60 and 70 pc, and Pound, Bania & Wilson (1990) have argued convincingly that the entire molecular complex must lie at nearly the same distance. In this direction, the edge of the local hot bubble is at a distance of at least 50pc, but probably less than 70pc (Welch et al. 1994), so that the L1457 complex must lie within or near its edge.

The L1457 molecular complex was first mapped in CO by Magnani, Blitz & Mundy (1985) in a search for high-latitude molecular clouds. (This work gives rise to the other common designation for these clouds, namely MBM 11 for L1453 and L1454, and MBM 12 for L1457 and L1458.) Ungerechts & Thaddeus (1987) included this molecular complex in their large-scale CO map of the Perseus, Taurus and Auriga regions. (The L1457 molecular complex is UT1 in their survey.) These surveys found a peculiar velocity structure with unusually broad spectral lines. Pound, Bania & Wilson (1990, hereafter PBW90) and Zimmerman & Ungerechts (1990, hereafter ZU90) mapped the L1457 molecular complex at angular resolution ~2' and ~4' respectively, PBW90 predominantly at ^{13}CO J=1-0 and ZU90 at ^{12}CO 1-0. They found a highly fragmented cloud of total mass $m_{H_2} \sim$ 30-200 $M_\odot$, with a large number of spatially and/or kinematically distinct fragments. Though most fragments had relatively modest linewidths, the combined effect leads to the large linewidths seen in the low-resolution maps. PBW90 and ZU90 also found that the fragments, with the possible exception of the L1457 core itself, are not gravitationally bound, even accounting for the external pressure from the hot "local bubble" gas (PBW90; ZU90). The molecular complex has the appearance of being a disrupted cloud. PBW90 have suggested that the molecular complex is being disrupted by the hot gas of the local bubble. Star formation could also have contributed to the disruption of the cloud (at least one and perhaps four other young stellar objects are present within the cloud complex (Magnani et al. 1995; Caillault, Magnani & Fryer 1995)).

The possible presence of disruptive UV radiation in the local bubble and the moderate star formation activity in the L1457 molecular complex both suggest the presence and importance of an extended component of atomic gas. However, except for a small HI map made by PBW90 toward the L1457 core, knowledge of the atomic component is lacking. In order to gain a fuller understanding of the L1457 molecular complex, we have mapped the large-scale ($\sim 8° \times 8°$, ~35' resolution) and small-scale ($\sim 3° \times 5°$, ~2' resolution) structure of the HI, and have obtained a larger map of ^{12}CO J=1-0 emission ($\sim 2° \times 4°$, ~2' resolution) covering most of the higher resolution HI map. In this paper we present the data, and compare the kinematics and morphology of the atomic, molecular, and dust (from IRAS COADD images) components of the L1457 complex.

2. OBSERVATIONS

HI observations were obtained using the Synthesis Telescope (ST) and the 26m single-dish telescope of the Dominion Radio Astrophysical Observatory[1]. The 26m telescope, operating at 1420.406 MHz, was used to map an $\sim 8^\circ \times 8^\circ$ field centered at (J2000) $2^h56^m27.5^s$ $+19^\circ57'04''$, sampling every 8'. (All coordinates listed in this paper are at epoch J2000.) The angular resolution of this telescope at this frequency is $\sim$35'. The data were obtained in 1992 August, and were calibrated by observations of the standard region S7 (Williams 1973). The backend was a 128-channel autocorrelator spectrometer, operating with a bandwidth of 0.25 MHz yielding a velocity resolution of each channel of 0.66 km s^{-1}.

Observations using the ST were made in 1992 November. The array consisted of seven 9m telescopes in an east-west configuration, observing simultaneously 21cm and 74cm continuum and the HI emission line at 1420.406 MHz. (The 74cm continuum observations, though available, were not used in this study.) By tracking a field center for 12 hours and moving the three mobile antennas between trackings, a complete *u-v* coverage is achieved with baselines from 12m to 600m at 4.3m intervals. Because of the limited number of correlators available at the time, we sought to enhance the sensitivity of our HI observations by acquiring both LHC and RHC polarizations, but limiting the maximum baseline to 300m. Maps were made by fourier-transforming the edited, calibrated, gridded visibilities. The angular resolution of the resultant images is (FWHM) $\sim$1.8' $\times$ 5' EW$\times$NS.

Extended HI structure, corresponding to interferometer spacings less than 12m, was extracted from the single-dish maps made using the 26m telescope. The ST and 26m maps were fourier-transformed, filtered and tapered in a complementary manner, and re-transformed. The ST data were corrected for the response of the primary beam of the 9m telescopes (i.e. polar diagram corrected), and the ST and 26m data were then added together. Thus the HI maps contain complete structure down to the size of the synthesized beam.

The maps in HI are in 128 radial velocity channels, with channel spacing 0.412 km s^{-1} (0.25 MHz total bandwidth) and resolution 0.66 km s^{-1}. The maps were later regridded to 0.65 km s^{-1} in order to match the channel spacings of the CO data (below). The RMS noise level of each channel was $\sim$1.0K. Each velocity map was corrected for continuum emission by subtracting out-of-band continuum from it (before adding the single-dish data). The HI maps were not cleaned because of the nearly complete *u-v* coverage and low sidelobe levels (<4%), and because the dynamic range within each map ($\lesssim$60) was insufficient to warrant cleaning.

To cover a large region surrounding the cloud complex, full aperture synthesis maps were made at two field centers, separated by $\sim 2^\circ$(i.e. at the $\sim$40% level). The two maps were regridded to a common sky projection and added together, weighting the overlapping regions by the square of the polar correction. In this way we have made maps of size $\sim 5^\circ \times 3^\circ$with a relatively constant noise level over much of the image.

The ^{12}CO J=1-0 (115.271 GHz) observations were acquired at the Five College Radio Astronomy Observatory 14m telescope on 1993 November 22-24. We used the 15-element QUARRY focal-plane array receiver operated in single sideband mode (Erikson et al. 1992), operating with a system temperature of 800-900K. The backend was a 15$\times$32-channel filterbank spectrometer with 250 kHz (0.65 km s^{-1}) channel spacings. The data were corrected to the T_R^* temperature scale (Kutner & Ulich 1981) by dividing by η_{FSS}=0.72, the forward spillover and scattering efficiency. When calculating mass, etc., a further correction

[1]The Dominion Radio Astrophysical Observatory is operated as a national facility by the Herzberg Institute for Astrophysics of the National Research Council of Canada.

for the coupling of the source with the telescope antenna pattern, η_C, must be applied to derive T_R. The value of η_C varies from 1 for a very extended source to 0.7 for a source much smaller than the error pattern. We have adopted η_c=0.8 as a compromise.

A $\sim 4^\circ \times 2^\circ$ region was mapped centered on the cloud complex. Integration times were typically 15 seconds on-source, 30 seconds reference, with one reference scan shared among several on-source spectra. The reference position was (J2000) $3^h04^m30.6^s + 19^\circ59'35"$, which was found to be free of CO emission over the 15 beams of the array receiver. Pointing and focus were checked 2-3 times per night, particularly just after sunset. Spectra were obtained every 50", which is the angular separation of the feedhorns and is just over the FWHM of the telescope at this frequency (~45"). The data were later smoothed to 2' resolution and the maps regridded to match that of the HI maps.

3. Results

The CO and HI data are shown as greyscale channel maps in Figures 2(a)-(l). HI and CO are displayed in the first and second columns respectively of each figure, using a fixed greyscale in all channels for each of HI and CO (a greyscale "wedge" is shown in Fig. 2(l)). In the third column we again show HI, but have stretched the contrast in order to highlight features in the image. Overlaid on these images are contours of the CO intensity.

3.1. HI

Atomic hydrogen emission can be seen in Fig. 2 from -9.8 to +13.61 km s^{-1}, a range of just under 24 km s^{-1}. There is much structure in all channels and at all sizescales. The most conspicuous features are extended filaments 1°to 4°long and $\lesssim$20' wide. An example can be seen at $V \sim -6.55$ km s^{-1}. Sometimes double, parallel filaments can be seen, for example at $V = -4.6$ km s^{-1}, at +7 to +8 km s^{-1} which becomes a single "braided" filament at 9-11 km s^{-1}, and another at $V \sim 9$ to 11 km s^{-1} near the south-west edge of the field extending off the image. This latter can also be seen in the large-scale images (Fig. 3). Most filaments are oriented roughly north-south and roughly parallel to the local magnetic field (Bhatt & Jain 1992; Leroy 1993a,b; Andersson & Wannier 1995), but a few fainter ones can also be seen extending roughly east-west (eg. a few in the southern half of the field at $+3 < V < 5$ km s^{-1}).

We can estimate the mass of HI in the vicinity of the CO. The integrated intensity $\int T_B dv$ was found at each point over the velocity interval -8 to +6 km s^{-1}, and this value was summed over a region defined by the CO. The total column density was derived from $N_{HI} = 1.823 \times 10^{18} \int T_B dv$ cm^{-2}, which assumes $\tau_{HI} \ll 1$. The mass of HI in the vicinity of the CO (assuming a distance of 65pc) was found to be ~48 $M_\odot$.

A few channel maps showing the large-scale ($\sim 8^\circ \times 8^\circ$, 35' resolution) HI structure are displayed in Figure 3. The major feature in this field is a structure $\sim 5^\circ \times 3^\circ$ (roughly EW × NS) from $-8 \lesssim V \lesssim +6$ km s^{-1}, and centered at $\sim 3^h, +21^\circ$. A velocity gradient is apparent in Fig. 3 running from west to east. At $V \sim 5.8$ km s^{-1}, this feature disappears entirely, and new structures appear at $V \gtrsim 7$ km s^{-1}. A map, integrated from -5.9 to +5.8 km s^{-1} and shown in Figure 4 (right), displays the large HI feature well. Also visible in this figure is a weaker extension to the HI feature, extending south $\sim 2^\circ$.

We can estimate the mass of HI in this large scale structure, by summing the integrated intensity (over the velocity interval -8 to +6 km s^{-1}) within a polygon defining the boundary of the HI structure, and

deriving the total column density as above. The total mass of HI in the entire structure was found to be 190 $M_\odot$.

3.2. CO

Part of the region has already been mapped by ZU90 and PBW90 at comparable resolution. We have covered a larger area (8 deg^2 compared to ~4.5 and ~2 deg^2 respectively), but find that both previous studies missed very little emission. Our CO data are displayed in Column 2 of Figure 2. We can see the major features described by ZU90 and PBW90, namely the rapidly changing structure between velocity channels, and the fragmentary nature of the CO emission. One feature which is readily apparent in our maps but much less evident in the ZU90 and PBW90 maps is the filamentary nature of the CO fragments at most velocities, most un- or barely-resolved but persisting for 2-4 channels and extending for a few arcmin.

Despite the clumpy, fragmentary nature of the CO, there is nonetheless a systematic velocity gradient, roughly west to east from ~-8 to +6 km s^{-1} over an angular distance of ~1.5°.

We have estimated the mass of the molecular gas in this complex by finding the integrated intensity $W_{^{12}CO} = \int T_R dv$ K km s^{-1} over the velocity interval -8 to +6 km s^{-1} and summing over the extent of the CO emission, and by assuming the relation $N_{H_2} = 2.6 \times 10^{20} W_{^{12}CO}$ cm^{-2} (Bloeman et al. 1986). From this, and assuming a distance of 65pc, we derive a mass of 140 $M_\odot$ for the molecular clouds. This compares to a mass of 200 $M_\odot$ found by ZU90 using a similar method. Based on their ^{13}CO observations and using an LTE calculation, PBW90 and ZU90 derive a mass of 30 $M_\odot$ and 40 $M_\odot$ respectively. Thus the mass of molecular gas is 30 - 200 $M_\odot$, but likely closer to the higher value.

4. Discussion

In Figure 1 the CO integrated intensity (from -8.5 to +5.8 km s^{-1}) is displayed as a contour map overlaid on a greyscale image of 100μm emission. This figure shows the extremely good correlation of molecular and dust emission. At larger scales Figure 4 compares HI, dust and CO. The bright 100μm emission which traces the CO so well, appears to be the southern "funnel-shaped" extension of a larger, ~ 5° × 3° structure or "plateau". This plateau correlates well with the large HI structure described previously (Fig. 4 (right)). Furthermore, a fainter southward extension of the HI structure corresponds to the bright 100μm emission. Thus the CO emission appears to be associated with large-scale HI.

At smaller scales (2' to 2°), there are remarkable correspondences of CO with HI. Column 3 of Fig. 2 displays directly these correspondences, which are complex. At $V \lesssim -9.8$ km s^{-1}, we see no CO and essentially no HI. From $-9 < V < -7$ km s^{-1}, CO is associated with an HI peak (which has an interesting filamentary structure) but is not coincident with it. The CO "horseshoe" described by PBW90 becomes evident at $V \gtrsim -7$ km s^{-1}, and at $V \sim -7$ km s^{-1} the vertex of the "horseshoe" appears to fit into the opening of a "v"-shaped HI structure. From $-7 < V < -4$ km s^{-1}, the CO is associated with a "double filament" of HI curving roughly from north to south. It is interesting that the HI associated with these filaments is brighter to the north and south of the CO, and that the CO appears to be bounded on the north and south by faint east-west filaments. A CO fragment can be seen south of the main CO complex at ~ $2^h58^m, +18°20'$ from -6 to -4 km s^{-1}, and seems to be located on the north edge of an HI filament running ESE to WNW. The HI from -4 to -1 km s^{-1} forms a roughly north-south ridge whose peak of

intensity is shifting gradually eastward. The CO continues to be found in the midst of this ridge. At $V > -1$ km s^{-1}, the HI ridge fades while the northern emission dominates, and a "border" of HI becomes apparent surrounding the CO. This is especially evident at ~ 0 km s^{-1}. The CO appears to become correlated, rather than anti-correlated, with HI at $V \gtrsim 1$ km s^{-1}, and at $3 \lesssim V \lesssim 6$ km s^{-1} the CO is located at the peak of the HI. CO disappears at $V \gtrsim 6$ km s^{-1}, while HI continues to display emission, mainly in a north-south filament. However, from the large-scale HI maps in Fig. 3, it can be seen that the HI emission at $V \gtrsim 6$ km s^{-1} is kinematically distinct from emission at $V < 6$ km s^{-1}, and is likely unrelated.

At the largest scales, the dust, molecular gas, and atomic gas appear to form a coherent structure of much larger size than the L1457 molecular complex alone. Furthermore, the HI and CO both span a similar velocity range with a west-to-east velocity gradient. The entire structure, which we will call the L1457 atomic/molecular complex, is approximately delineated by the $100\mu m$ peak and plateau emission seen in Figure 4, and assuming a distance to the complex of 65 pc, is $\sim 6.8 \times 4.5$ pc in extent. (The CO alone is $\sim 1\times$ 2 pc in extent, EW $\times$ NS.) The molecular component of this atomic/molecular complex takes up $\sim$ 20 - 50% of the total mass.

Ungerechts & Thaddeus (1987) have mapped the large-scale CO in this vicinity, and found another molecular cloud, UT 2, $\lesssim 3°$ from the L1457 molecular complex (their UT 1). We have indicated its position on Fig. 4. Interestingly, it is located within the $100\mu m$ "plateau" and on the north-east edge of the HI structure. Its velocity of +1.2 km s^{-1} (Ungerechts & Thaddeus 1987) is also the same as that of the HI in its vicinity, and is likely related to it. Thus we believe that UT 2 is part of the L1457 atomic/molecular complex.

A molecular cloud in the presence of the interstellar UV field will be heated and photodissociated on the outside surface leading to the formation of an envelope or halo of warm atomic gas surrounding the molecular cloud (Hollenbach, Werner & Salpeter 1971; Federman, Glassgold & Kwan 1979). Such structures were first detected by Wannier, Lichten & Morris (1983), and their results were extended in a series of related papers (Wannier et al. 1991; Andersson, Wannier & Morris 1991; Andersson, Roger & Wannier 1992). The Perseus B3-B5 molecular cloud complex is an example of molecular clouds possessing extended, expanding, limb-brightened, atomic halos (Andersson, Roger & Wannier 1992; Moriarty-Schieven, Wannier & Andersson 1997). In the case of L1457, an atomic halo is present, but not so extended as in other molecular clouds. At velocities greater than -2 km s^{-1}, the filamentary nature of the HI forms a bright but narrow rim surrounding the CO cloud. This rim is especially evident at V $\sim$ 0 km s^{-1} and +2 km s^{-1}. Here it is less than 10' thick (0.2 pc). This is in marked contrast to the halo surrounding B5, which is more than 1.5 pc in thickness. At velocities less than -2 km s^{-1}, HI clearly surrounds the CO and is associated with it, but there is no similar sign of limb-brightening around the molecular emission. Instead the CO seems to form part of the HI structure (which is mostly filamentary at these velocities). Such a narrow (and at V $\lesssim$ -1 km s^{-1}) ill-defined halo may indicate that the expected halo is being disturbed by external pressure or some other mechanism.

From their observations, PBW90 and ZU90 showed that, with the possible exception of the L1457 clump itself, the molecular clouds in the complex are not gravitationally bound. They furthermore found that the external pressure due to the hot gas in the local bubble, estimated to be P/k $\sim 10^4$ cm^{-3} K (Cox & Reynolds 1987), was too small to balance the internal gas pressure of the dense clumps, estimated to be P/k $\sim 10^5$ cm^{-3} K (PBW90; ZU90), and so concluded that the molecular clouds were breaking up. One component of external pressure not adequately addressed was the HI surrounding and coexisting with the CO. Assuming a cylindrical geometry of diameter $\sim 1.5°$ and height $\sim 2.5°$ containing an HI mass of ~ 50 M$_\odot$, we derive an average density of $n_{HI} \sim 300$ cm^{-3}. Although the temperature of HI is not known, it is likely of order 100K, yielding a pressure P/k $\sim$ 3 $\times$ 10^4 cm^{-3} K, probably insufficient to contain the molecular gas. It should

be noted that this average HI density is large, and is usually associated with molecular cloud densities. The average HI density in the northern "plateau" is $\sim$50 cm^{-3} assuming a cylinder of diameter $\sim$6.8 pc and height 4.5 pc.

The remarkable structure of the L1457 atomic/molecular complex, both at large and small scales, suggests that the complex has recently been compressed leading to the collapse of half the HI cloud and the formation of some of the molecular clouds. At the largest scales, the complex is made up of two distinct parts. The large, diffuse, northern section is made up mostly of HI, while the southern extension, though taking up roughly half of the mass of the complex, is small and remarkably dense with a concave "funnel" shape. The east and west edges of the "funnel" form concave, semi-circular walls meeting (and even extending beyond) the cusp or south-point, which in the 100μm image (Fig. 4a) look like the walls of bubbles. Indeed, within these "bubbles", both the 100μm and large-scale HI images (Fig. 4) show marked emission minima.

Despite the differences in size and density, the north and south parts of the complex have a remarkably similar velocity structure. Both have the same range of velocity ($\sim$-8 to $\sim$+5 km s^{-1}) and the same roughly west-to-east velocity gradient, but the south's gradient extends over $\sim$1.5°while the that of the north over $\sim$5°.

The HI/CO structure at small scales (Fig. 2a-l) is also intriguing. The expected extended atomic haloes of molecular clouds are instead narrow or poorly defined. Rather the structure of the HI is most often filamentary in the southern extension. The filaments are long, narrow, and slightly curved, and are often seen as two parallel lines which appear to merge at some velocities. These filaments are most likely sheets seen edge-on. Their orientation, usually roughly north-south, and length of $\sim$1°-4°, means that they run parallel to and nearly the length of the east and west walls of the southern extension. Indeed, these structures are reminiscent of the sheets and filaments seen in supernova remnants. The molecular gas is not gravitationally bound, and there is insufficient external pressure, including that from the HI, to contain it.

Star formation processes and external pressure from the hot bubble gas are unlikely to have created the disturbed, dense southern region of this complex. Nevertheless the morphology and kinematics suggest that it has experienced a recent large compression event. A cartoon of this scenario is shown in Fig. 5. As a result of this compression, the southern part of the HI cloud collapsed, forming the filaments, increasing the density and perhaps leading to the formation of much of the molecular gas. (Some molecular gas must have pre-existed the collapse because of the 1-5 young stellar objects which are presumably $\sim 10^6$ years old, associated with the cloud (Magnani et al. 1995; Caillault et al. 1995).) PBW90 have suggested that the supernova which is presumed to have created the local hot bubble $\sim 10^5$ years ago (Cox & Reynolds 1987) could easily have provided the conditions necessary to create the molecular cloud complex out, as we have seen, of an originally much larger HI structure. This atomic/molecular complex was thus likely created $\lesssim 10^5$ years ago in a supernova blast (Chevalier 1977), and is continuing to be disturbed by its echo. It is unclear if the L1457 complex is within the local hot bubble, however. This scenario would suggest that it is within the bubble.

5. Summary

L1457, a high latitude ($b \sim -34°$) dark cloud complex, is the closest known molecular cloud at a distance of 65pc, and may be located within the local hot bubble.

We have mapped HI and ^{12}CO J=1-0 emission over a large region including the L1457 molecular cloud

complex, covering a region 8°× 8°at 35' resolution and ~3°× 5°at 2' × 5' resolution in HI emission, and a region 2°× 4°at 2' resolution in CO.

We find that there is an extended component of atomic gas, clearly associated with the molecular complex, and comparable to it in total mass.

The structure of the HI in the vicinity of the molecular gas is intriguing. The most conspicuous features are extended filaments 1°- 4°(1-5pc) in length and $\lesssim$20' (0.2pc) wide. These filaments are often double, and may be sheets of HI seen edge-on. The orientations of most are roughly north-south. This is approximately parallel to the local magnetic field, but also parallel to the east and west sides of the molecular complex.

Warm, limb-brightened atomic halos around the molecular clouds are ill-defined at some velocities or are very narrow at others. This may indicate that the atomic halos are being disturbed by external pressure, perhaps from the hot gas in the local bubble.

The molecular clouds form a small "funnel-shaped" southern extension ~ 1.5°× 2°in size, of a much larger structure ~ 5° × 3° in size, which we are calling the L1457 atomic/molecular complex. The larger northern part of the complex is mostly HI. Roughly half of the mass of the complex is in molecular gas. The northern and southern parts of the complex have the same velocity range (-8 to +6 km s^{-1}) and west-to-east gradient, but the south velocity gradient is over a much shorter distance.

The structure of the atomic/molecular complex at large- and small-scale suggests that the southern end has recently been compressed to form the molecular clouds. A supernova ~10^5 years ago which is believed to have created the local hot bubble may have been the cause.

We would like to thank our anonymous referee for helpful suggestions. GMS was supported by a Research Associateship from the National Research Council of Canada.

REFERENCES

Andersson, B-G, Roger, R. S., & Wannier, P. G. 1992, A&A, 260, 355

Andersson, B-G, & Wannier, P. G. 1995, ApJ, 443, L49

Andersson, B-G, Wannier, P. G. & Morris, M., 1991, ApJ, 366, 464

Bhatt, H. C., & Jain, S. K. 1992, MNRAS, 257, 57

Bloeman, J. B. G. M., Strong, A. W., Blitz, L., Cohen, R. S., Dame, T. M., Grabelsky, D. A., Hermsen, W., Lebrun, F., Mayer-Hasselwander, H. A., & Thaddeus, P. 1986, A&A, 154, 25

Caillault, J.-P., Magnani, L., & Fryer, C. 1995, ApJ, 441, 261

Chevalier, R. A. 1977, ARA&A, 15, 175

Cox, D. P., & Reynolds, R. J. 1987, ARA&A, 25, 303

Erikson, N. R., Goldsmith, P. F., Novak, G., Grosslein, R. M., Viscuso, P. J., Erikson, R. B., & Predmore, C. R. 1992, IEEE Trans. on Microwave Theory and Techniques, 40, 1

Federman, S. R., Glassgold, A. E., & Kwan, J. 1979, ApJ, 227, 466

Hollenbach, D. J., Werner, M. W., & Salpeter, E. E. 1971, ApJ, 163, 165

Hobbs, L. M., Blitz, L., & Magnani, L. 1986, ApJ, 306, L109

Hobbs, L. M., Blitz, L., Penrase, B. E., Magnani, L., & Welty, D. E. 1988, ApJ, 327, 356

Kutner, M. L., & Ulich, B. L. 1981, ApJ, 250, 341

Leroy, J. L. 1993a, A&AS, 101, 551

Leroy, J. L. 1993b, A&A, 274, 203

Lynds, B. T. 1963, ApJS, 7, 1

Magnani, L., Blitz, L., & Mundy, L. 1985, ApJ, 295, 402

Magnani, L., Caillault, J-P., Buchalter, A., & Beichman, C. A. 1995, ApJS, 95, 159

McCammon, D., Burrows, D. N., Sanders, W. T., & Kraushaar, W. L. 1983, ApJ, 269, 107

Moriarty-Schieven, G. H., Wannier, P. G., & Andersson, B-G. 1997, in preparation

Pound, M. W., Bania, T. M., & Wilson, R. W. 1990, ApJ, 351, 165 (PBW90)

Ungerechts, H., & Thaddeus, P. 1987, ApJS, 63, 645

Wannier, P. G., Andersson, B-G, Morris, M. & Lichten, S., 1991, ApJS, 75, 987

Wannier, P. G., Lichten, S. M., & Morris, M. 1983, ApJ, 268, 727

Welch, B. Y., Craig, N., Vedder, P. W., & Vallerga, J. V. 1994, ApJ, 437, 638

Williams, D. R. W. 1973, A&AS, 8, 505

Zimmerman, T., & Ungerechts, H. 1990, A&A, 238, 337 (ZU90)

Fig. 1.— "Road map" of the L1457 molecular cloud complex showing CO integrated intensity (contours every 7 K km s^{-1}) and a greyscale image of the 100μm emission. The greyscale is linear from 5 MJy sr^{-1} (white) to 42.5 MJy sr^{-1} (black).

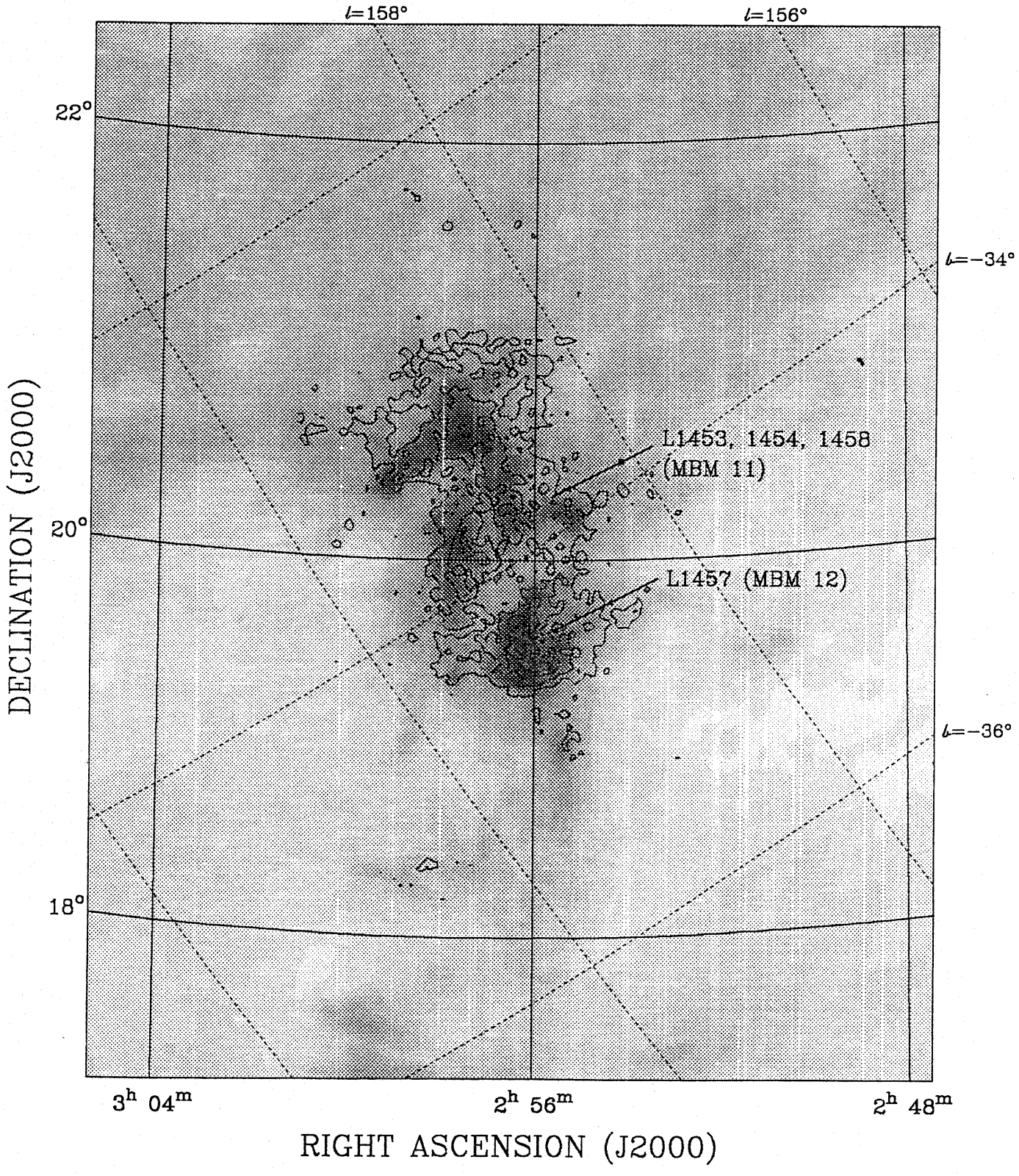

Fig. 2.— Greyscale images of HI channel maps at 2' × 5' resolution (EW×NS) (Column 1; linear greyscale from 0 K (white) to 85 K (black), "wedge" on final figure)), CO (Column 2; linear greyscale from (T_R^*) -0.25 K (white) to 6.75 K (black), "wedge" on final figure)), and CO contours (1K, 3K, 5K contour levels) on HI emission contrast-enhanced Column 3).

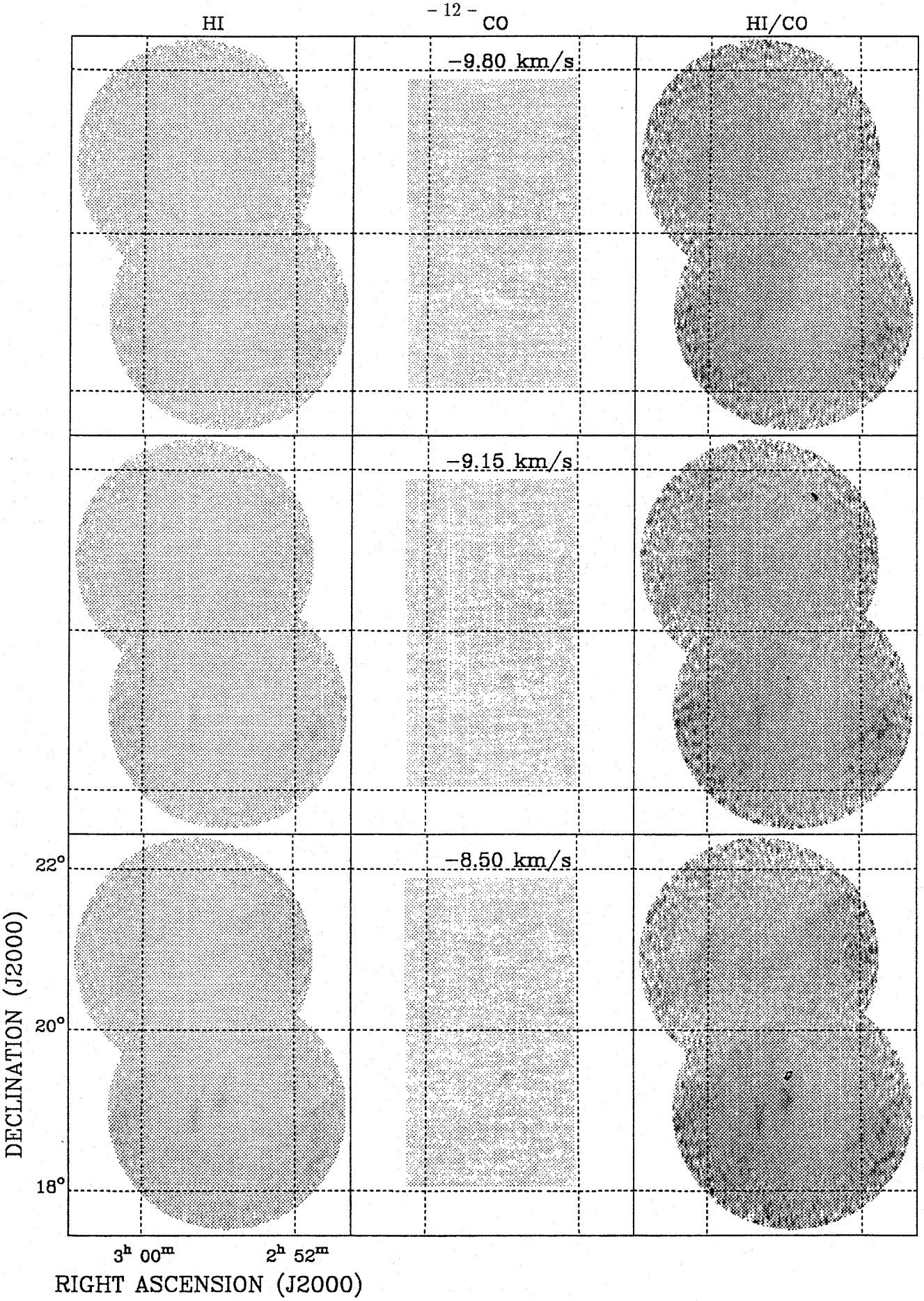
HI
CO
HI/CO
−9.80 km/s
−9.15 km/s
−8.50 km/s
22°
20°
18°
DECLINATION (J2000)
3h 00m
2h 52m
RIGHT ASCENSION (J2000)

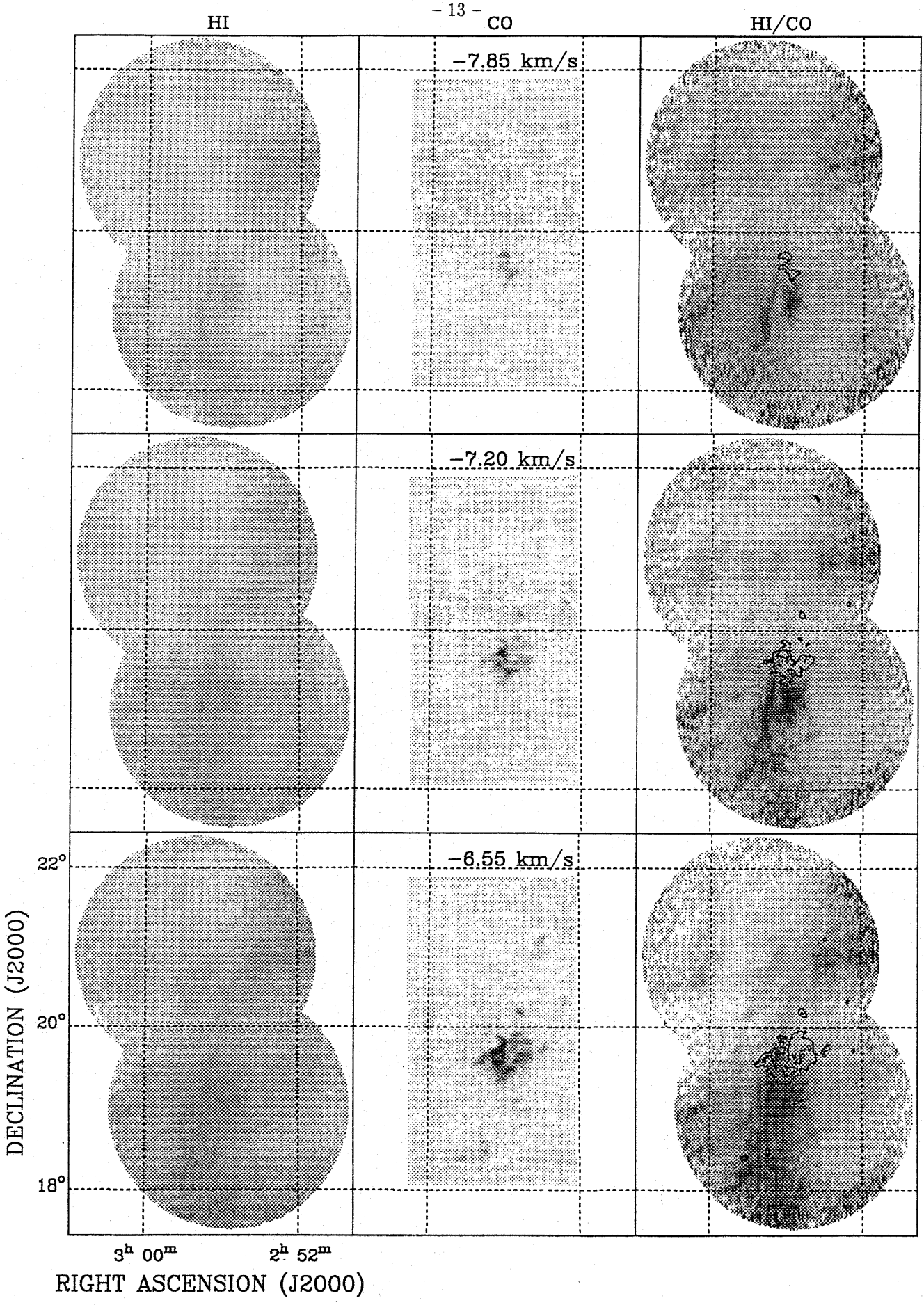
HI
CO
HI/CO
−7.85 km/s
−7.20 km/s
−6.55 km/s
22°
20°
18°
DECLINATION (J2000)
3h 00m
2h 52m
RIGHT ASCENSION (J2000)

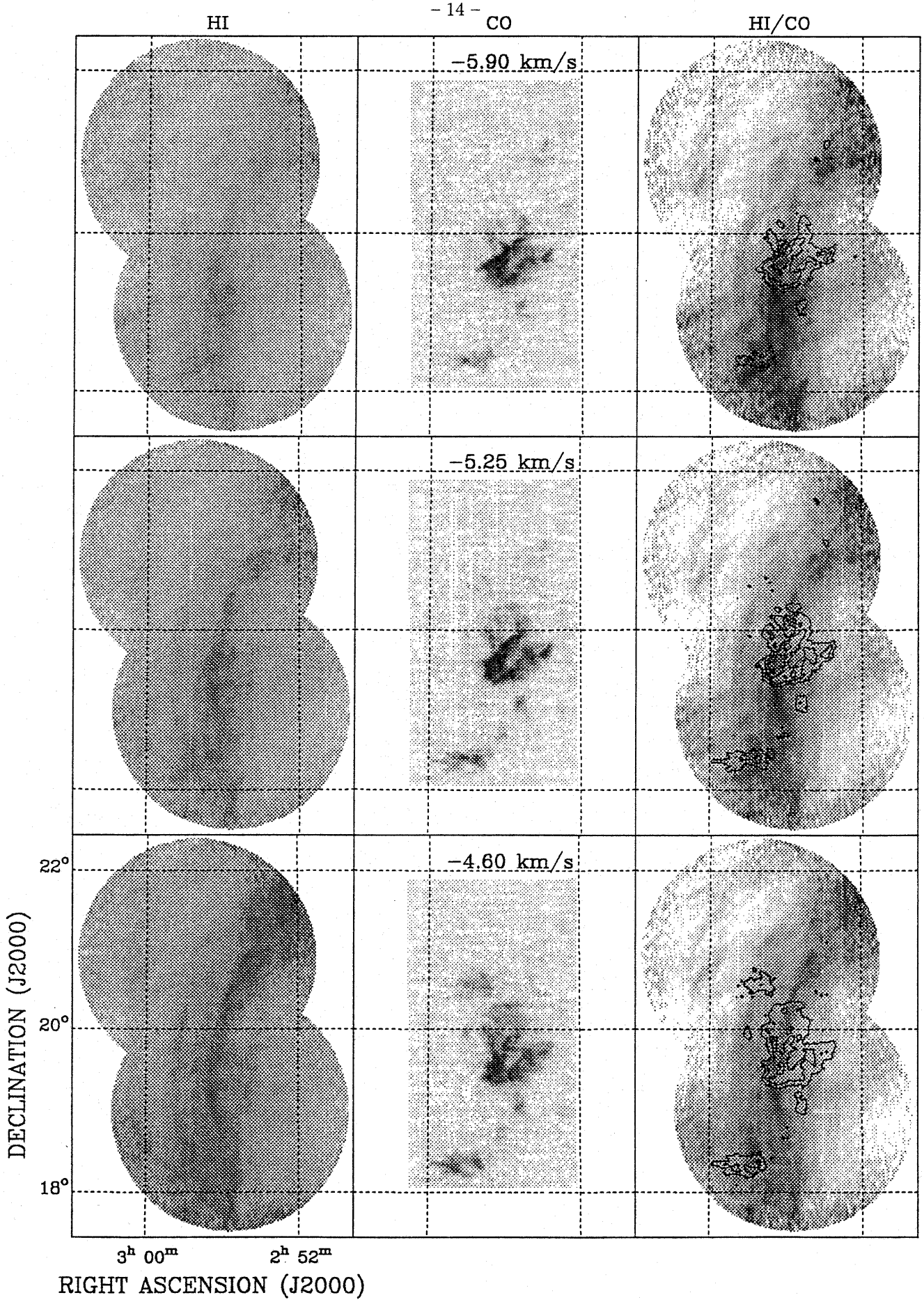
HI
CO
HI/CO
−5.90 km/s
−5.25 km/s
−4.60 km/s
22°
20°
18°
DECLINATION (J2000)
3h 00m
2h 52m
RIGHT ASCENSION (J2000)

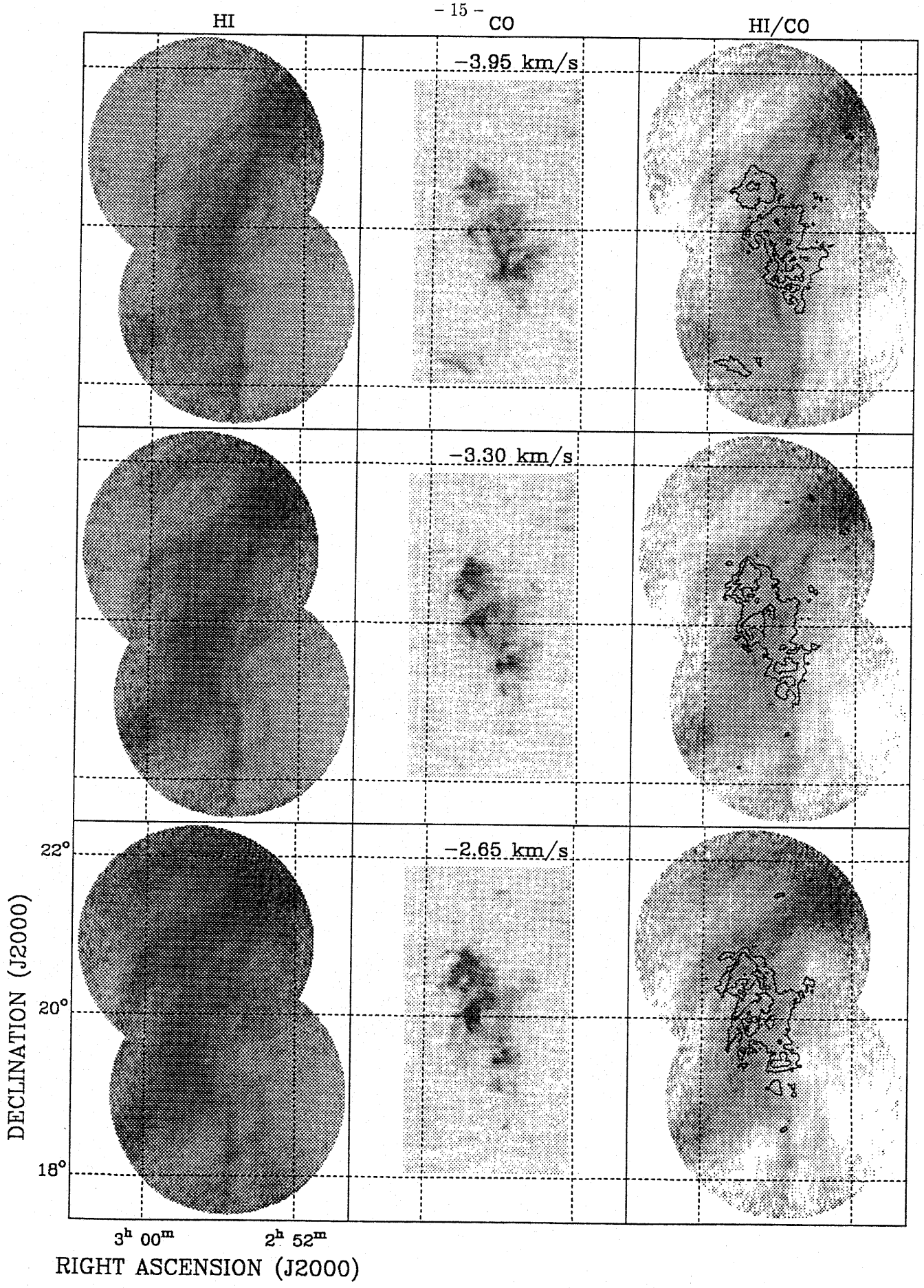
HI
CO
HI/CO
−3.95 km/s
−3.30 km/s
−2.65 km/s
22°
20°
18°
DECLINATION (J2000)
3h 00m
2h 52m
RIGHT ASCENSION (J2000)

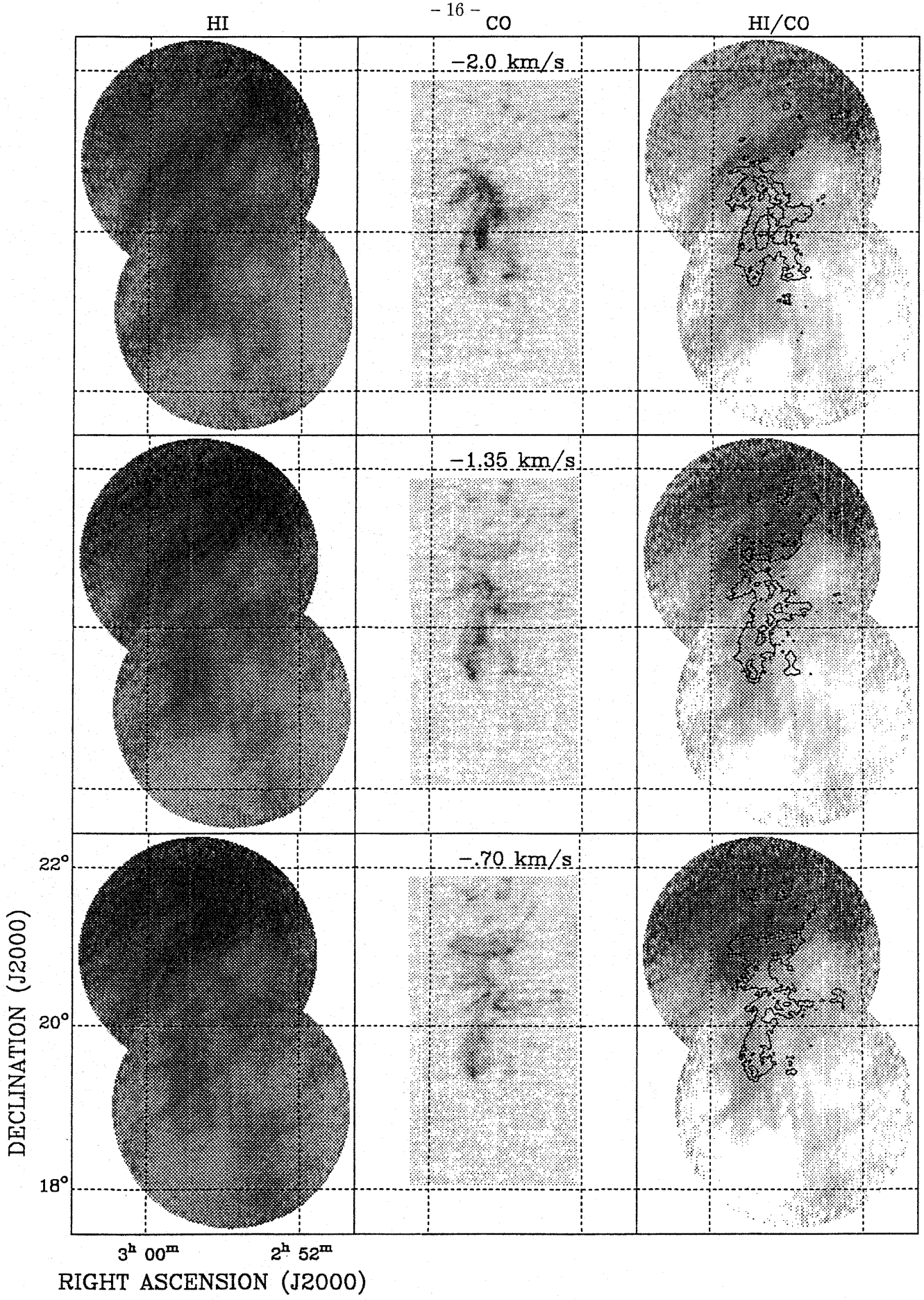
HI
CO
HI/CO
−2.0 km/s
−1.35 km/s
−.70 km/s
22°
20°
18°
DECLINATION (J2000)
3h 00m
2h 52m
RIGHT ASCENSION (J2000)

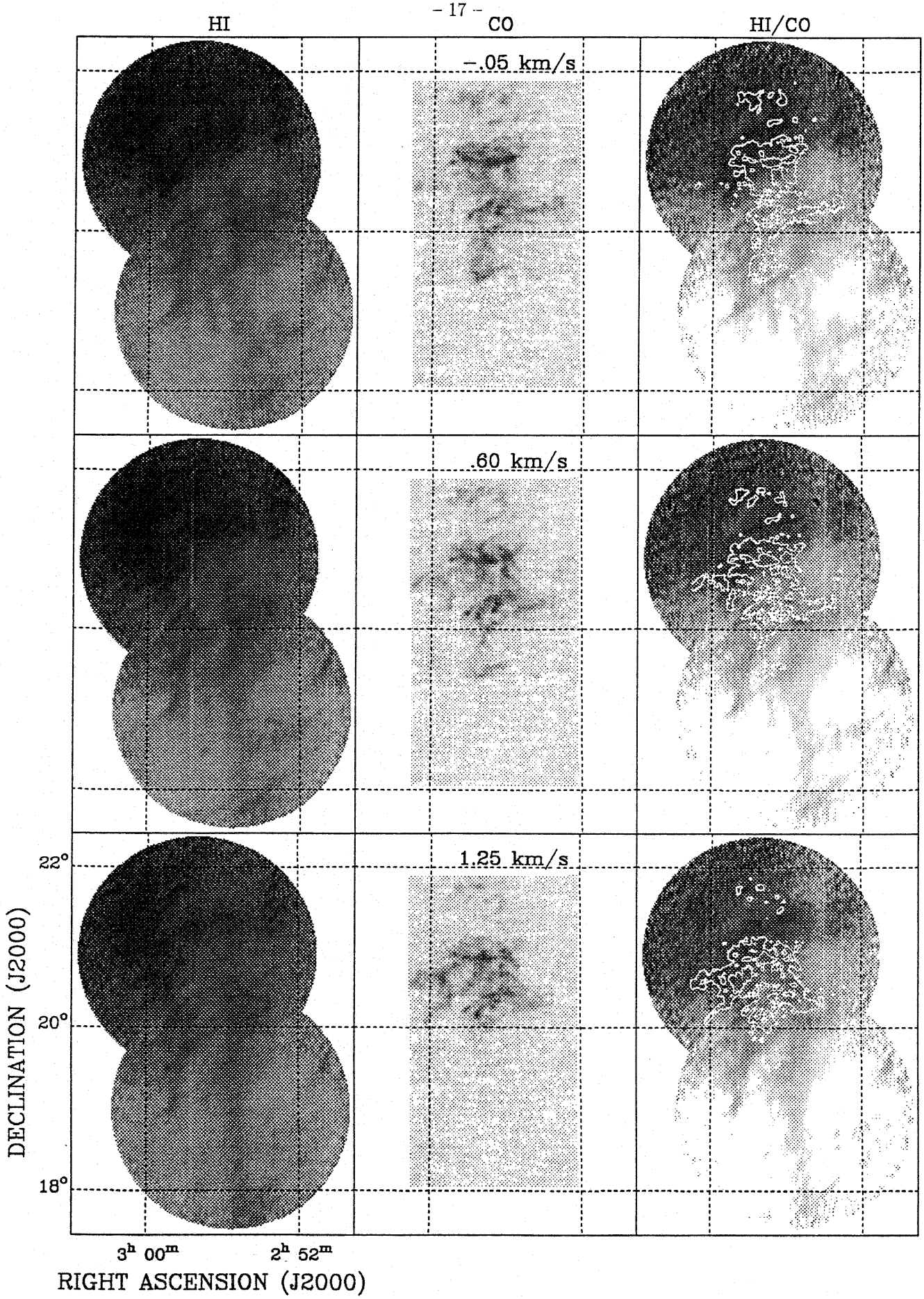
HI
CO
HI/CO
-.05 km/s
.60 km/s
1.25 km/s
22°
20°
18°
DECLINATION (J2000)
3h 00m
2h 52m
RIGHT ASCENSION (J2000)

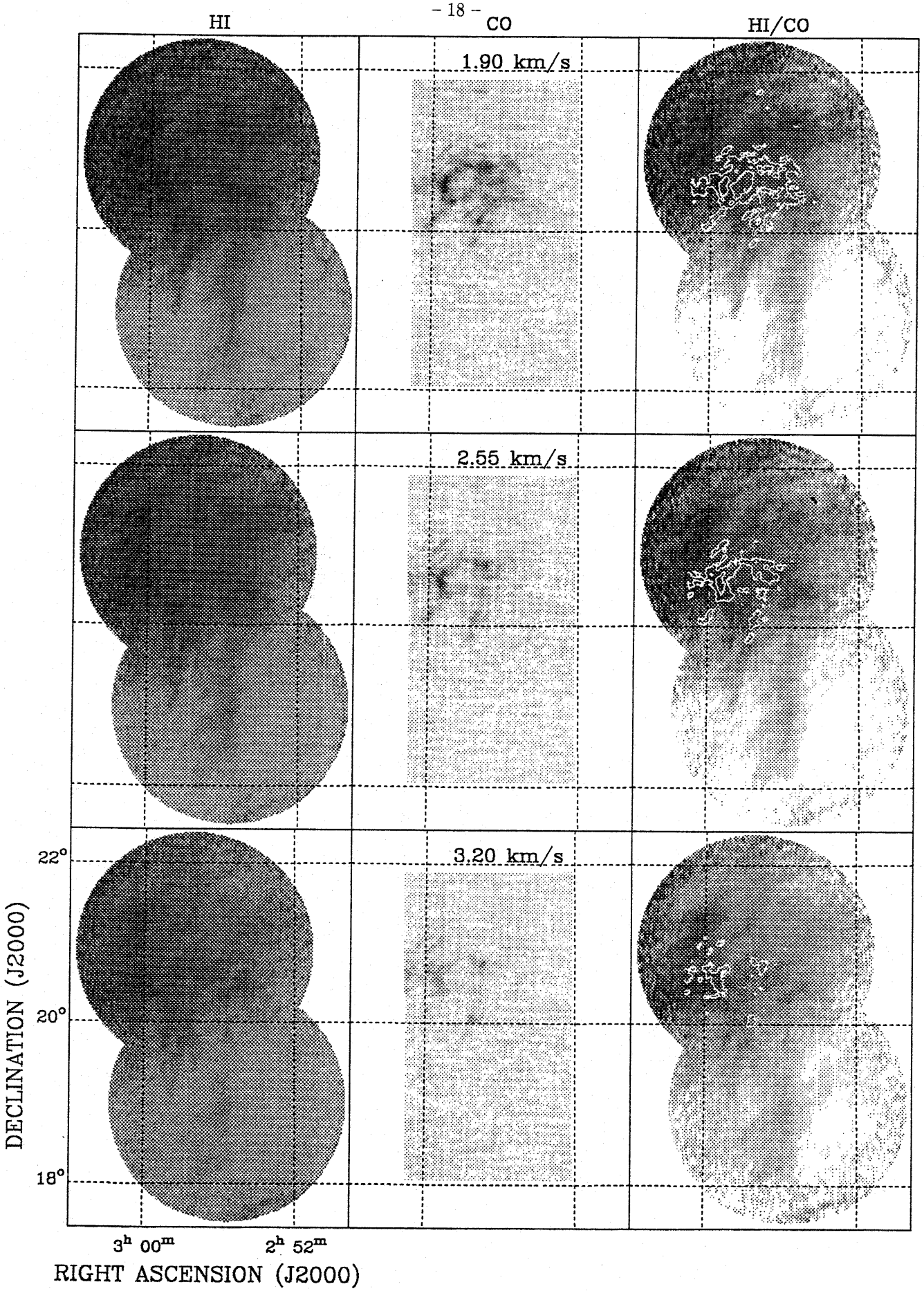
HI
CO
HI/CO
1.90 km/s
2.55 km/s
3.20 km/s
22°
20°
18°
DECLINATION (J2000)
3h 00m
2h 52m
RIGHT ASCENSION (J2000)

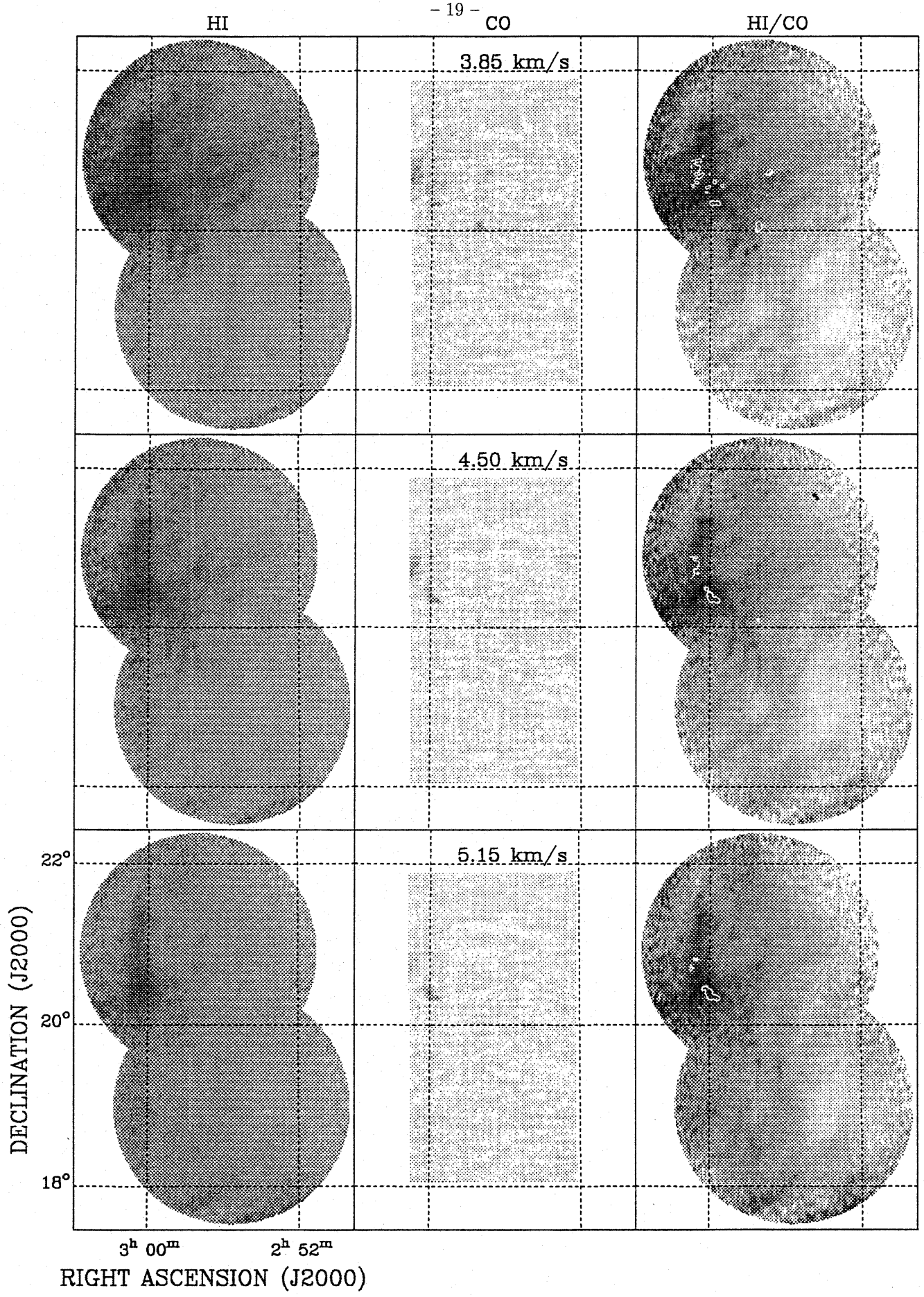
HI
CO
HI/CO
3.85 km/s
4.50 km/s
5.15 km/s
22°
20°
18°
DECLINATION (J2000)
3h 00m
2h 52m
RIGHT ASCENSION (J2000)

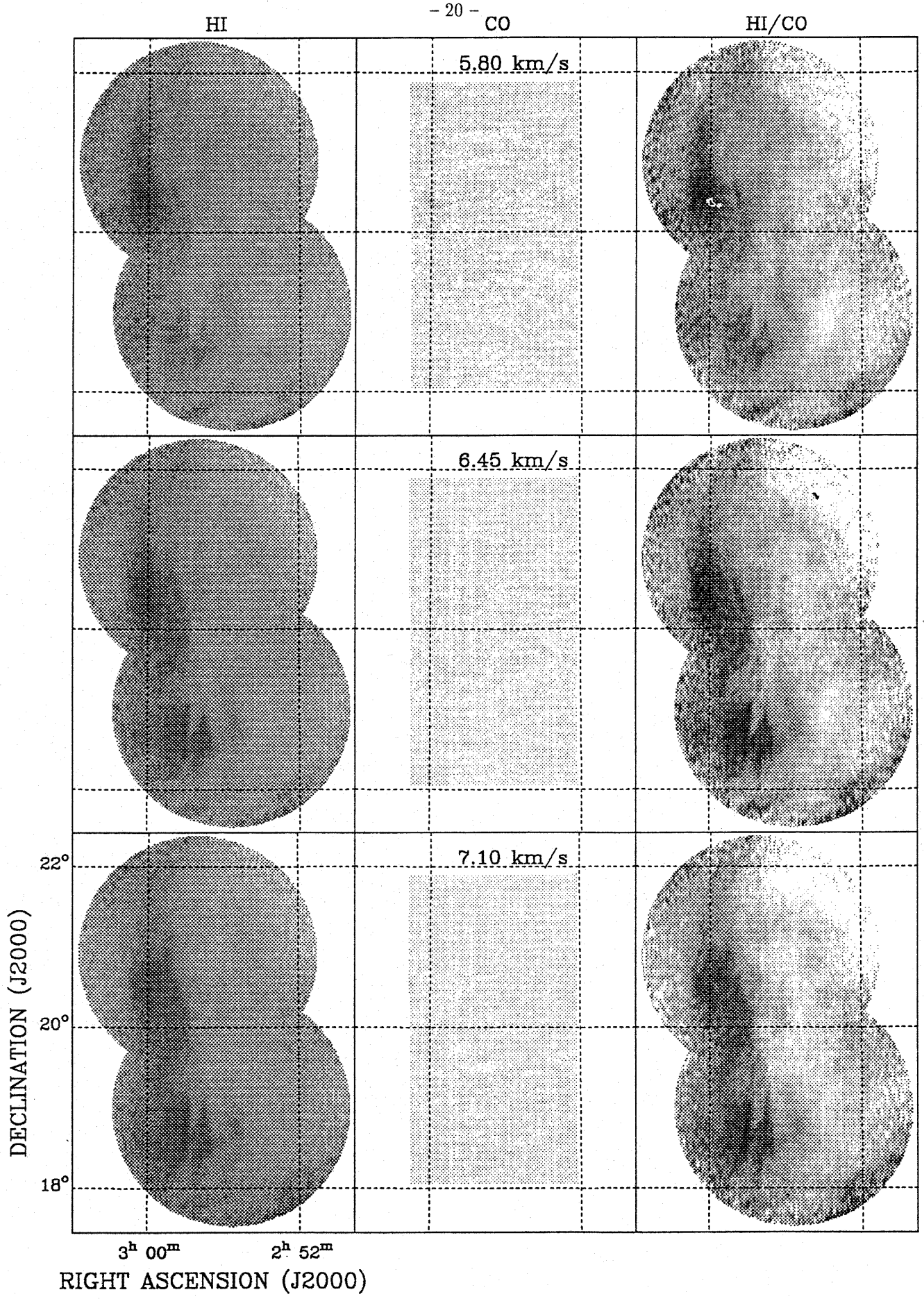
HI
CO
HI/CO
5.80 km/s
6.45 km/s
7.10 km/s
22°
20°
18°
DECLINATION (J2000)
3h 00m
2h 52m
RIGHT ASCENSION (J2000)

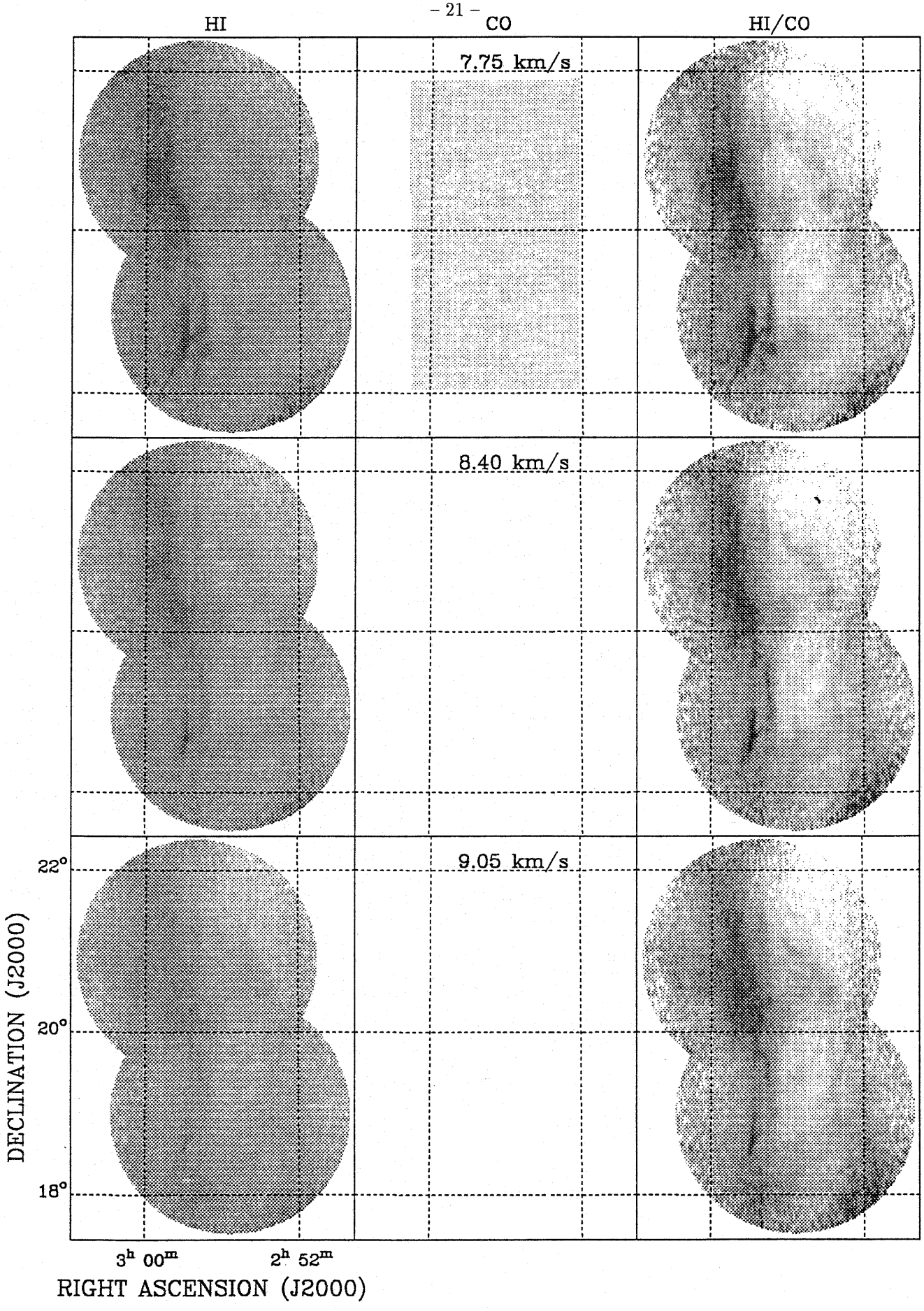
HI
CO
HI/CO
7.75 km/s
8.40 km/s
9.05 km/s
22°
20°
18°
DECLINATION (J2000)
3h 00m
2h 52m
RIGHT ASCENSION (J2000)

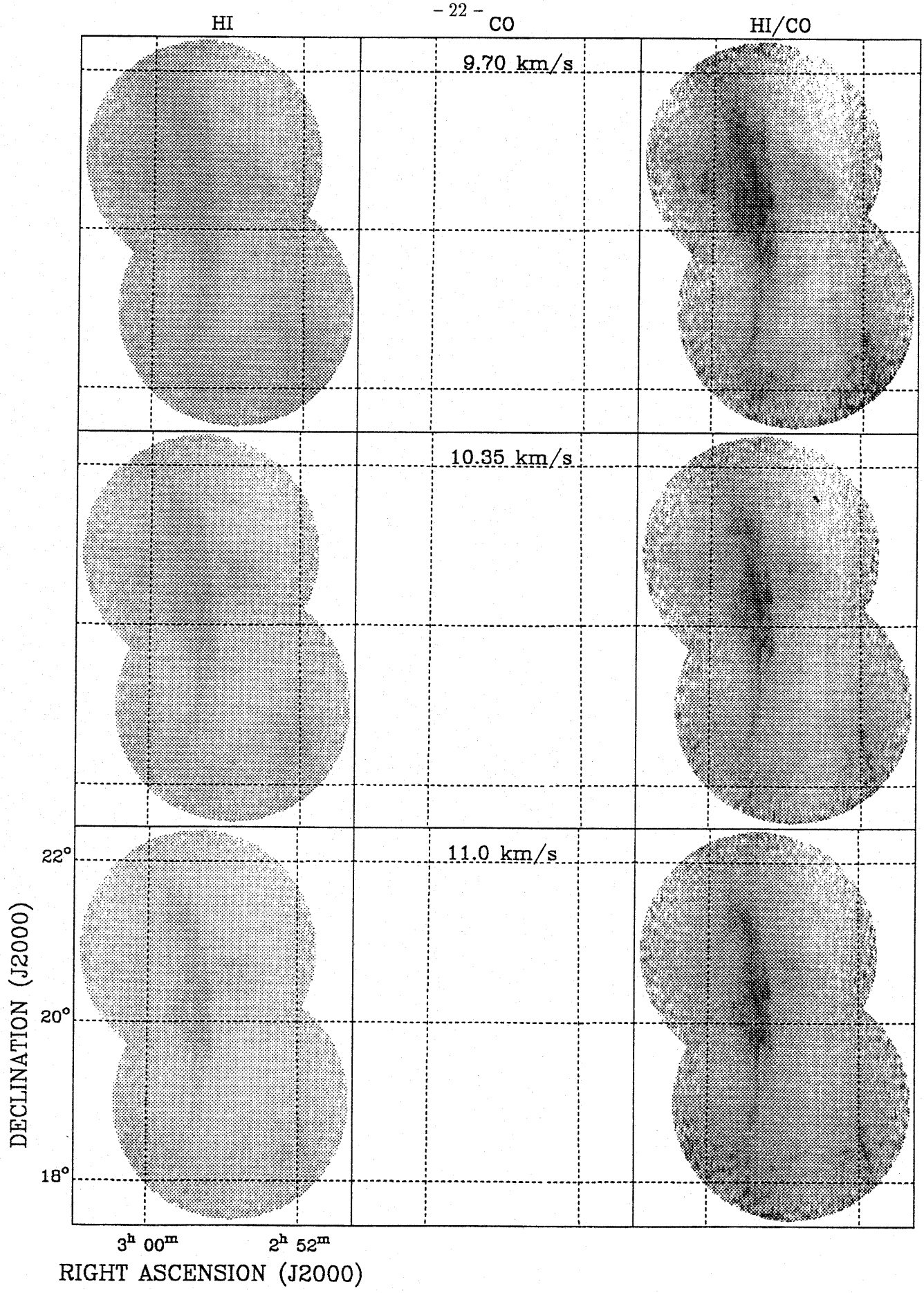
HI
CO
HI/CO
9.70 km/s
10.35 km/s
11.0 km/s
22°
20°
18°
DECLINATION (J2000)
3h 00m
2h 52m
RIGHT ASCENSION (J2000)

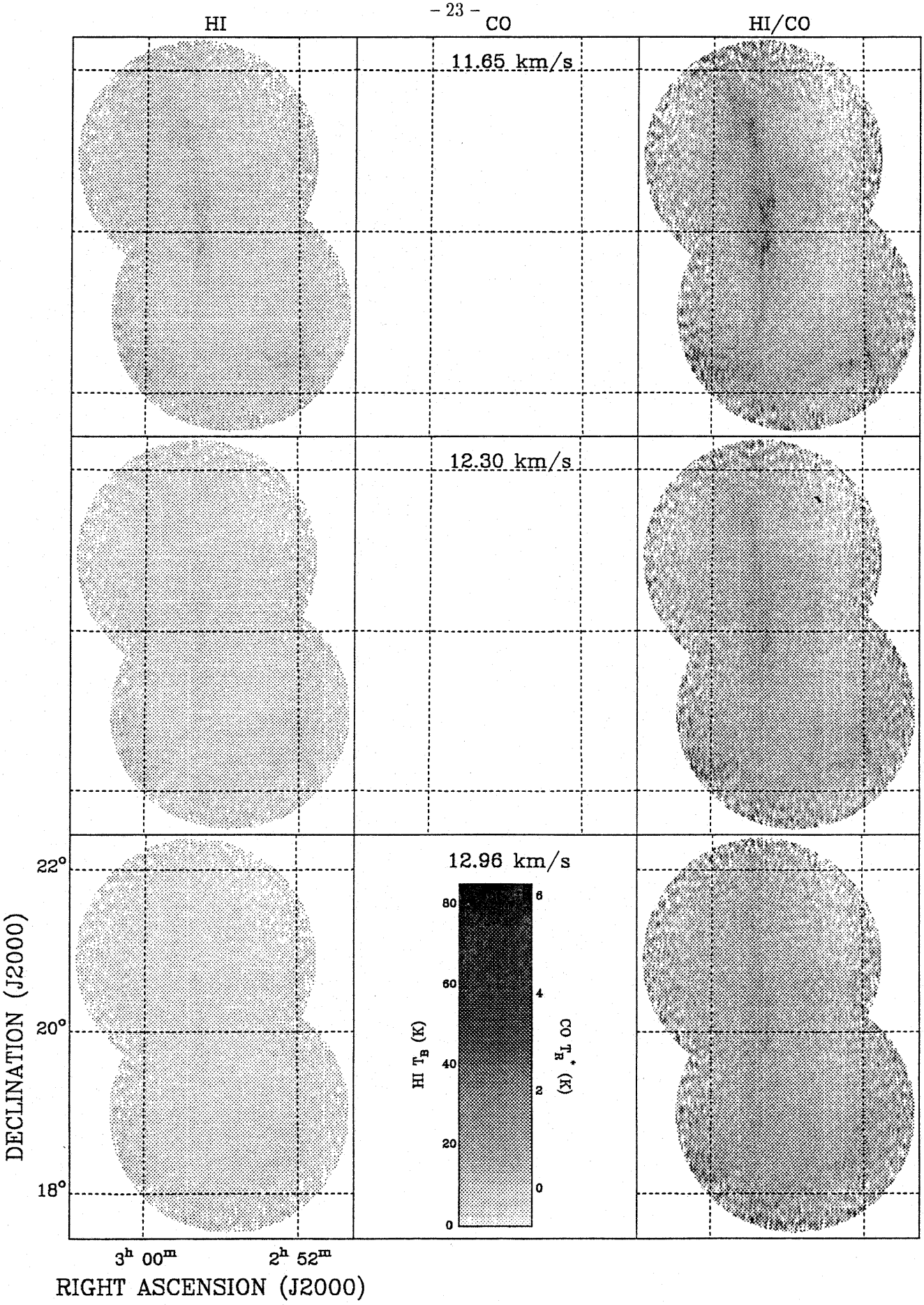
HI
CO
HI/CO
11.65 km/s
12.30 km/s
12.96 km/s
22°
20°
18°
DECLINATION (J2000)
3h 00m
2h 52m
RIGHT ASCENSION (J2000)
HI T_B (K)
CO T_R^* (K)
80
60
40
20
0
6
4
2
0

Fig. 3.— Greyscale images of HI channel maps of large-scale emission at 35' resolution. Greyscale is linear from 0 K (white) to 70 K (black). Contours are $100\mu m$ emission (contour levels every 6 MJy sr^{-1}). The dashed box indicates the extent of the high resolution (~2') HI maps.

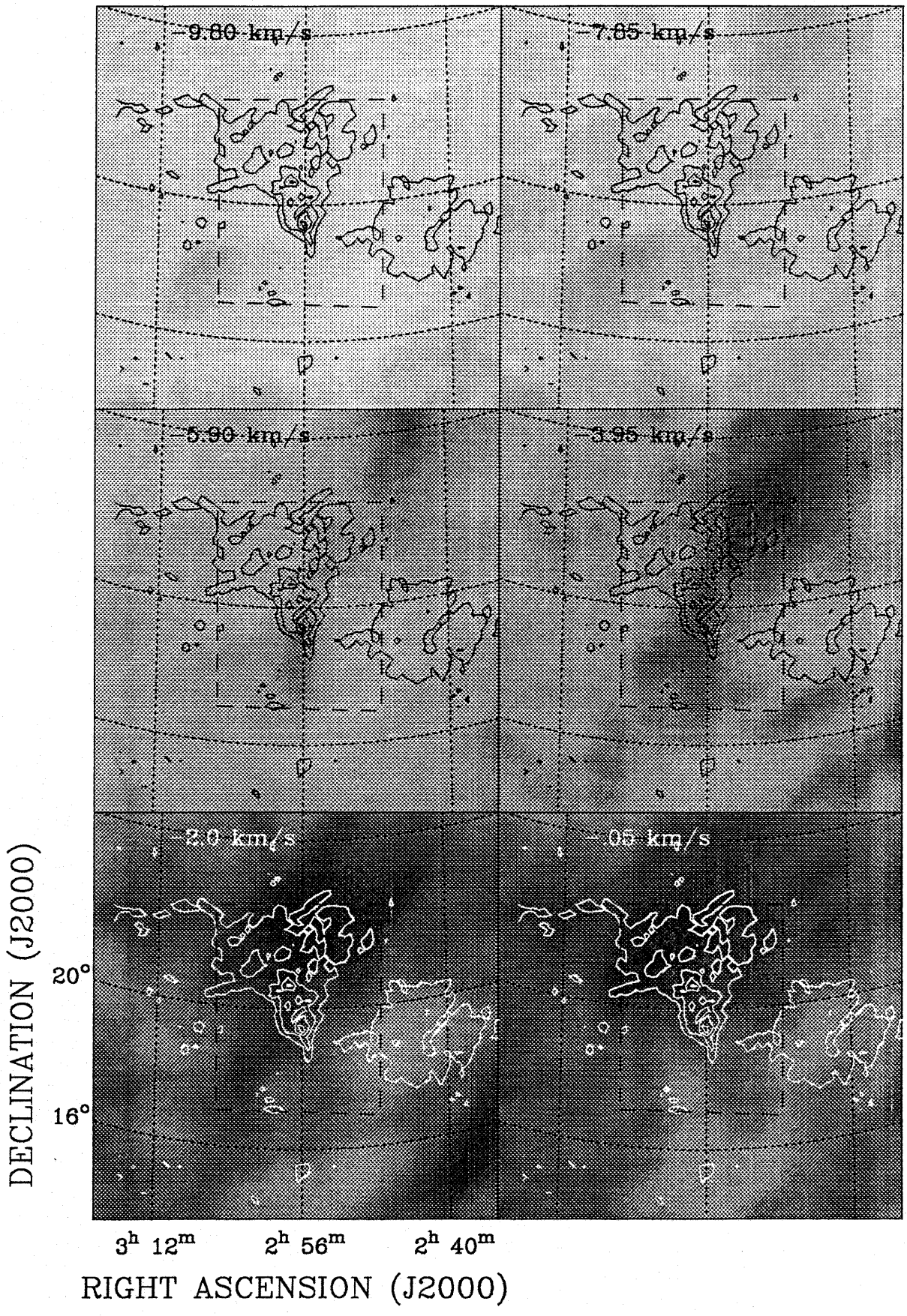
9.80 km/s
7.85 km/s
5.90 km/s
3.95 km/s
2.0 km/s
0.0 km/s
DECLINATION (J2000)
20°
16°
3h 12m
2h 56m
2h 40m
RIGHT ASCENSION (J2000)

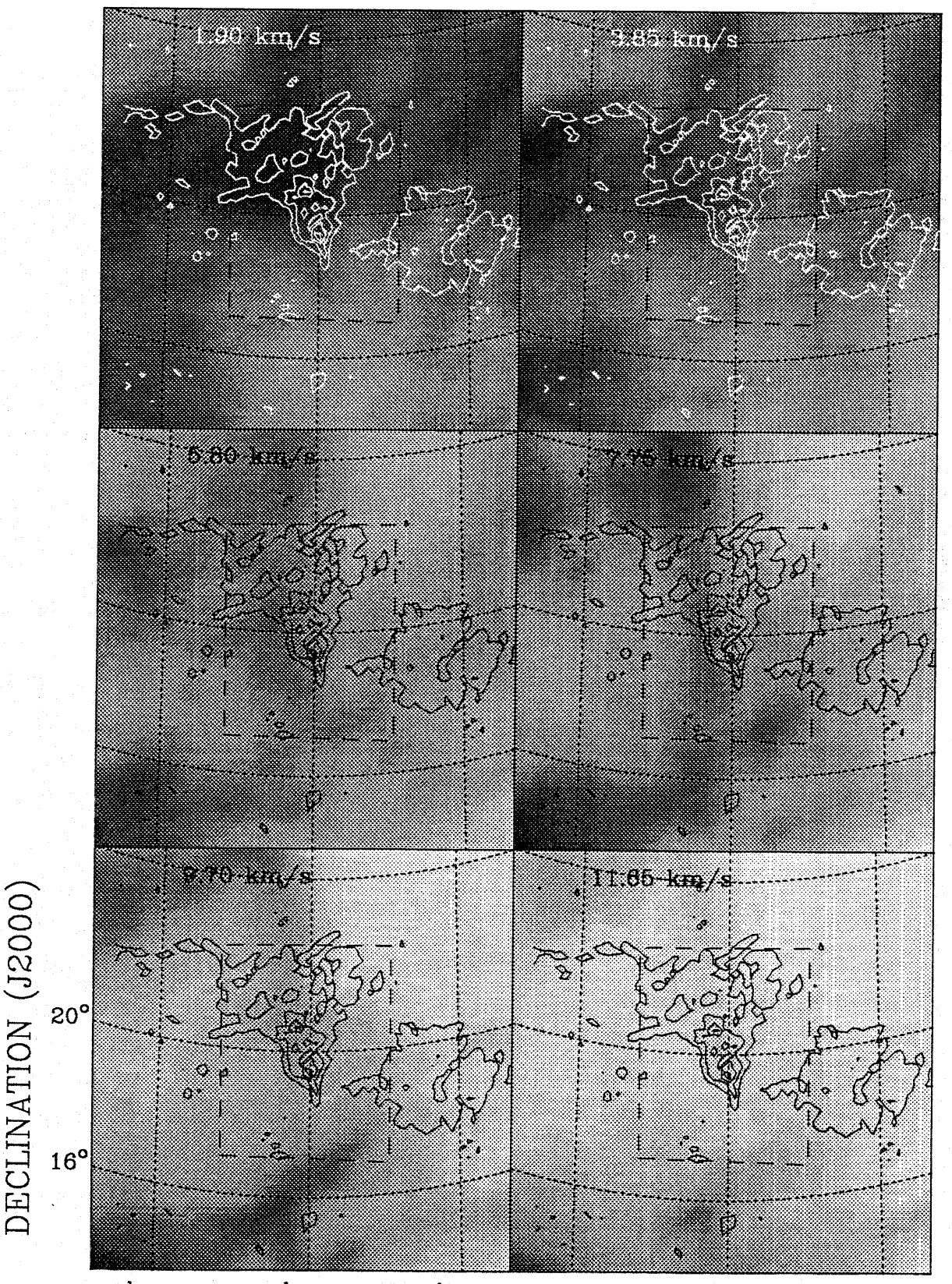
1.90 km/s
3.85 km/s
5.80 km/s
7.75 km/s
9.70 km/s
11.65 km/s
DECLINATION (J2000)
20°
16°
3h 12m
2h 56m
2h 40m
RIGHT ASCENSION (J2000)

Fig. 4.— Large-scale dust, molecular gas, and atomic gas emission. (a) Greyscale of $100\mu m$ (linear from 4.5 MJy sr^{-1} (white) to 39 MJy sr^{-1} (black)). Overlaid is the 8 K km s^{-1} contour of the integrated CO intensity. Also shown in the location of the UT 2 molecular cloud (Ungerechts & Thaddeus 1987). (b) Greyscale of large-scale integrated intensity HI emission (linear from 20 K (white) to 42 K (black)). Overlaid are contours of $100\mu m$ emission (every 6 MJy sr^{-1}).

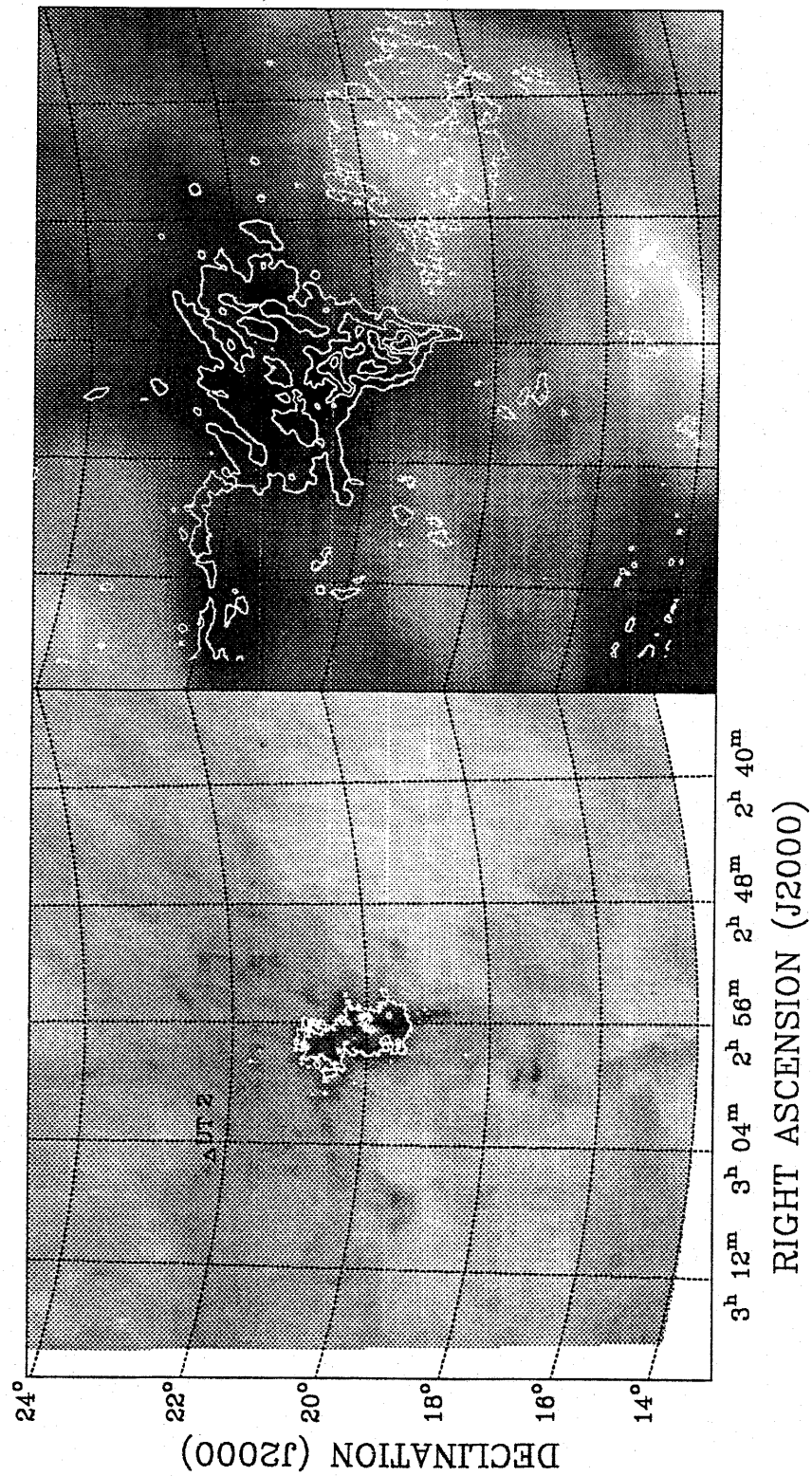

Fig. 5.— Sketch representing the L1457 atomic/molecular complex.